Dang-Jun Yu* and Jie-Fang Zhang

Rogue Wave and Breather Structures with "High Frequency" and "Low Frequency" in $\mathcal{PT}$-Symmetric Nonlinear Couplers with Gain and Loss

DOI 10.1515/zna-2016-0229
Received June 9, 2016; accepted August 1, 2016; previously published online August 26, 2016

Abstract: Based on the modified Darboux transformation method, starting from zero solution and the plane wave solution, the hierarchies of rational solutions and breather solutions with "high frequency" and "low frequency" of the coupled nonlinear Schrödinger equation in parity-time symmetric nonlinear couplers with gain and loss are constructed, respectively. From these results, some basic characteristics of multi-rogue waves and multi-breathers are studied. Based on the property of rogue wave as the "quantum" of pattern structure in rogue wave hierarchy, we further study the novel structures of the superposed Akhmediev breathers, Kuznetsov-Ma solitons and their combined structures. It is expected that these results may give new insight into the context of the optical communications and Bose-Einstein condensations.

Keywords: Modified Darboux Transformation; $\mathcal{PT}$-Symmetric Nonlinear Couplers; Rogue Waves; Superposed Breathers.

1 Introduction

Nowadays, a vast variety of methods have been developed to obtain solitonic solutions of a given nonlinear partial differential equation [1–8]. Rogue waves (RWs, also known as freak waves, monster waves, killer waves, extreme waves, and abnormal waves) are relatively large and spontaneous waves which is firstly recorded and studied in oceanography [9]. Generally speaking, RWs sometimes can be several times higher than the average wave crests. Nowadays, RWs have flourished into a research area of great importance and interest in nonlinear optics [10], plasmas [11] and Bose-Einstein condensations [12], etc.

As we all know, rational solutions (also Peregrine solitons [13]) as theoretical prototypes to describe RWs have been extensively studied. Akhmediev's group [14, 15] obtained rational solutions of the standard nonlinear Schrödinger equation (NLSE) and higher order NLSE. More recently, the time-periodic Kuznetsov [16] or Ma [17] (KM) soliton and the space-periodic Akhmediev breather (AB) [18] have become two prototypes to theoretically describe RWs [19, 20]. Rogue wave solutions of some generalised nonautonomous nonlinear equations in the nonlinear inhomogeneous fiber have also been discussed [21, 22]. However, all works [13–22] were done without considering parity-time ($\mathcal{PT}$) symmetric medium.

The $\mathcal{PT}$ symmetry firstly appeared in quantum mechanics since Bender and coworkers [23] in 1998 pointed that non-Hermitian Hamiltonians exhibit entirely real spectra, provided that they respect both the parity and time-reversal symmetries. In optics, the first experiment of the $\mathcal{PT}$ symmetry was implemented in coupled optical waveguides with balanced gain and loss [24]. Spatiotemporal localizations in (3+1) -dimensional $\mathcal{PT}$-symmetric and strongly nonlocal nonlinear media were studied [25]. The $\mathcal{PT}$ symmetry can also realised as a pair of linearly coupled optical waveguide (also called a dimer) composed of a passive waveguide carrying linear loss and its active counterpart imparted with a matched compensating gain [26]. Recently, breathers in $\mathcal{PT}$-symmetric optical couplers were discussed [27]. Moreover, nonlinear tunnelling effect of combined KM soliton in (3+1)-dimensional $\mathcal{PT}$-symmetric inhomogeneous nonlinear couplers with gain and loss was also investigated [28]. However, to the best of our knowledge, multi-RWs and multi-breathers have not been studied in $\mathcal{PT}$-symmetric coupled optical waveguides although single breathers [27] and KM solitons [28] in $\mathcal{PT}$-symmetric couplers have been reported.

In this article, we obtain the hierarchies of rational solutions and breather solutions with "high frequency" and "low frequency" of the coupled NLSE in $\mathcal{PT}$ symmetric

***Corresponding author: Dang-Jun Yu,** Jinhua Polytechnic, Jinhua, Zhejiang 321007, P.R. China, E-mail: zjydj2015@126.com
Jie-Fang Zhang: School of Electronics Information, Zhejiang University of Media and Communications, Hangzhou 310018, P.R.China

nonlinear couplers with gain and loss via the modified Darboux transformation (DT) method. With the help of these results, we discuss some basic properties of multi-RWs and multi-breathers. Based on the property of RW as the "quantum" of pattern structure in RW hierarchy, we further study the novel structures of the superposed ABs, KM solitons and their combined structures.

2 Model and Lax Pair

The dynamics of light beams and pulses in $\mathcal{PT}$-symmetric nonlinear couplers with gain and loss can be described by the following NLSE [29]

$$\begin{aligned} &\mathrm{i}u_z + u_{xx} + 2|u|^2 u = -v + \mathrm{i}\gamma u, \\ &\mathrm{i}v_z + v_{xx} + 2|v|^2 v = -u - \mathrm{i}\gamma v, \end{aligned} \tag{1}$$

where z stands for time and x for the spatial coordinate in the frame moving with the pulse group velocity [30]. $u(z, x)$ and $v(z, x)$ are two normalised complex mode fields. Alternatively, this model can also describe one-dimensional array of $\mathcal{PT}$-symmetric coupled waveguides with z and x being dimensionless propagation and transverse coordinates [31, 32]. In this case, the initial-value problem corresponds to an optical beam shone into the waveguides' input at given $z = z_i$. Here the Kerr nonlinearity coefficients in the two waveguides (coefficients in front of $|u|^2u$ and $|v|^2v$) have equal. They are self-focusing nonlinearity in the case of beams and the anomalous dispersion with positive Kerr nonlinearity in the case of pulses. The first terms in the right-hand sides of (1) denote the coupling between the modes propagating in the two waveguides. The second terms in the right-hand sides account for the gain in one and loss in the other waveguide, which describes the $\mathcal{PT}$-balanced gain in the first equation of (1) and loss in the second equation of (1). The gain and loss coefficients are taken equal to conform to the $\mathcal{PT}$-symmetry condition [33]. In optics, this setting can be realised using a system of two lossy parallel-coupled waveguides, doped by gain-providing atoms, in which only one waveguide is pumped by the external source of light which supplies the gain.

When the gain/loss term is small enough, such as $\gamma \le 1$, the energy through linear coupling is transferred from the core with gain to the lossy one, and modes can be excited in the system by input beams but do not arise spontaneously. Without loss of generality, it is convenient to make a change of variable with $\gamma = \sin(\theta)$. Along the idea of [29], we make the following change of variables

$$\begin{aligned} &u(x, z) = U(z, x)\exp[\mathrm{i}(\omega z - \theta)], \\ &v(x, z) = V(z, x)\exp(\mathrm{i}\omega z). \end{aligned} \tag{2}$$

Inserting this relation into (1), and assuming $U = V = \psi$ yields

$$\mathrm{i}\psi_z + \psi_{xx} + 2|\psi|^2\psi - a^2\psi = 0, \tag{3}$$

with $a^2 = \omega - \cos(\theta)$.

In solution (2), $u(x, z)$ and $v(x, z)$ have same amplitude, however, possess different phase. $\gamma = \sin(\theta)$ defines two different angles, that is, $\theta = \arcsin\gamma \in [0, \pi/2]$ and $\theta = \pi - \arcsin\gamma \in [\pi/2, \pi]$. Accordingly, (3) describes two separate invariant manifolds of the system (1). Both invariant manifolds are characterised by the Hamiltonian evolution. Moreover, two families of solutions are also distinguished by the sign of $\cos(\theta)$. One has $\cos(\theta) = \sqrt{1-\gamma^2}$ denoting the corresponding solitons by $\{u_+, v_+\}$ and another has $\cos(\theta) = -\sqrt{1-\gamma^2}$ denoting the corresponding solitons by $\{u_-, v_-\}$.

From $a^2 = \omega - \cos(\theta)$, we know that the frequency ω of solution has the expression $\omega = a^2 + \cos(\theta)$. Thus the frequency ω of $\{u_+, v_+\}$ is $\omega = a^2 + \sqrt{1-\gamma^2} > a^2$, but the frequency ω of $\{u_-, v_-\}$ is $\omega = a^2 - \sqrt{1-\gamma^2} < a^2$. It is clear that the frequency ω of $\{u_+, v_+\}$ is higher than that of $\{u_-, v_-\}$. Therefore, we can name two solitons after the "high frequency" and "low frequency" solutions. Similar low- and high-frequency solitons have been analysed before [27, 29, 31, 32]. Note that authors only studied "high frequency" solitons in [31]. Also note that these "high frequency" and "low frequency" solitons have not been reported in the system without $\mathcal{PT}$-symmetric terms. In this meaning, the transformation from coupled NLSE with $\mathcal{PT}$-symmetric terms into a standard NLSE provides a way to study the "high frequency" and "low frequency" solitons in $\mathcal{PT}$-symmetric system.

Equation (3) is a condition of compatibility of the two following linear equations

$$\begin{aligned} &\mathbf{R}_x = \lambda\mathbf{J}\mathbf{R} + \mathbf{U}\mathbf{R}, \\ &\mathbf{R}_z = 2\lambda^2\mathbf{J}\mathbf{R} + 2\lambda\mathbf{U}\mathbf{R} + \frac{1}{2}\mathbf{V}\mathbf{R} + \mathbf{M}\mathbf{R}, \end{aligned} \tag{4}$$

where the column matrix $\mathbf{R}$ satisfies

$$\mathbf{R} = \begin{pmatrix} r \\ s \end{pmatrix}, \tag{5}$$

with two linear complex functions $r = r(z, x)$, $s = s(z, x)$ and the square matrices $\mathbf{U}$, $\mathbf{J}$, $\mathbf{V}$ and $\mathbf{M}$ are in the form

$$\mathbf{U} = \begin{pmatrix} 0 & i\psi^* \\ \mathrm{i}\psi & 0 \end{pmatrix}, \mathbf{J} = \begin{pmatrix} \mathrm{i} & 0 \\ 0 & -\mathrm{i} \end{pmatrix}, \tag{6}$$

$$\mathbf{V}=2\begin{pmatrix}-\mathrm{i}|\psi|^2 & \psi_x^* \\ -\psi_x & \mathrm{i}|\psi|^2\end{pmatrix},\ \mathbf{M}=\begin{pmatrix}\mathrm{i}a^2/2 & 0 \\ 0 & -\mathrm{i}a^2/2\end{pmatrix}, \tag{7}$$

where * denotes the complex conjugate and λ is a complex eigenvalue. It is easy to verify that Eq. (3) can be recovered from the compatibility condition $\mathbf{R}_{xz}=\mathbf{R}_{zx}$. According to the relations above, we can easily write down the scalar set of equations for the linear equations (4) as follows

$$\begin{aligned} r_x &= \mathrm{i}\psi^* s+\mathrm{i}\lambda r,\\ s_x &= \mathrm{i}\psi r-\mathrm{i}\lambda s,\\ r_z &= \mathrm{i}2\lambda^2 r+\mathrm{i}2\lambda\psi^* s-\mathrm{i}|\psi|^2 r+\psi_x^* s+\frac{\mathrm{i}}{2}ra^2,\\ s_z &= -\mathrm{i}2\lambda^2 s+\mathrm{i}2\lambda\psi r+\mathrm{i}|\psi|^2 s-\psi_x r-\frac{\mathrm{i}}{2}sa^2. \end{aligned} \tag{8}$$

3 RW Solutions and Structures

According to the modified DT technique in [14, 15], the one-to-one correspondence between the solution ψ of (3), and the solutions r and s of the linear system (4) or (8) is constructed, thus solution ψ of (3) can be derived by solving the linear system, which is easier to be solved. The modified DT technique starts from the trivial solutions of (3), such as the zero solution $\psi_0=0$ or the plane-wave solution $\psi_0=\exp(iz)$. Then via the following scheme $\psi_0\to(r_1, s_1)\to\psi_1\to(r_2, s_2)\to\psi_2\to(r_3, s_3)\to u_3\ldots$, the trivial "seeding" solutions of (3) to generate more complicated solutions, and the relation between the given "seeding" solution and the next level solution is expressed as

$$\psi_j=\psi_{j-1}+\frac{2(\lambda^*-\lambda)s_j r_j^*}{|r_j|^2+|s_j|^2}, \tag{9}$$

where the index j is related to the order of the solution in the hierarchy, ψ_{j-1} is the solution of the previous step while ψ_j is the solution of the next step. Different "seeding" solutions results in different complicated solutions. For example, the zero "seeding" solution allows us to construct the hierarchy of multisoliton solutions, while the plane-wave "seeding" solution leads to the hierarchy of solutions related to modulation instability or rational solutions [14, 15]. For rational solutions, the complex eigenvalue $\lambda=\mathrm{i}$.

In the following, we start from the seeding solution $\psi_0=\exp[\mathrm{i}(2-a^2)z]$ to obtain RW solutions. We split the functions $\psi(z, x)$, r_j and s_j into their real (with the subscript r) and imaginary (with the subscript i) parts and factor out the exponentials:

$$\begin{aligned} \psi(z, x) &= [\phi_{jr}(z, x)+\mathrm{i}\phi_{ji}(z, x)]\exp[\mathrm{i}(2-a^2)z],\\ r_j(z, x) &= [r_{jr}(z, x)+\mathrm{i}zr_{ji}(z, x)]\exp[-\mathrm{i}(2-a^2)z/2],\\ s_j(z, x) &= [s_{jr}(z, x)+izs_{ji}(z, x)]\exp[\mathrm{i}(2-a^2)z/2]. \end{aligned} \tag{10}$$

Substituting these expressions (10) into the linear equations (8) yields

$$\begin{aligned} &\frac{\partial r_{jr}}{\partial x}+r_{jr}=z\phi_{j-1,i}\tilde{r}_{ji}-\phi_{j-1,r}\tilde{r}_{jr},\\ &z\frac{\partial r_{ji}}{\partial x}+zr_{ji}=z\phi_{j-1,r}\tilde{r}_{ji}+\phi_{j-1,i}\tilde{r}_{jr},\\ &\frac{\partial r_{jr}}{\partial z}-z(1+\phi_{j-1,r}^2+\phi_{j-1,i}^2)r_{ji}=\\ &\quad z\left(\frac{\partial\phi_{j-1,r}}{\partial x}-2\phi_{j-1,r}\right)\tilde{r}_{ji}+\left(\frac{\partial\phi_{j-1,i}}{\partial x}-2\phi_{j-1,i}\right)\tilde{r}_{jr},\\ &z\frac{\partial r_{ji}}{\partial z}+(1+\phi_{j-1,r}^2+\phi_{j-1,i}^2)r_{jr}=\\ &\quad z\left(2\phi_{j-1,i}-\frac{\partial\phi_{j-1,i}}{\partial x}\right)\tilde{r}_{ji}+\left(\frac{\partial\phi_{j-1,r}}{\partial x}-2\phi_{j-1,r}\right)\tilde{r}_{jr}, \end{aligned} \tag{11}$$

where $\tilde{r}_{jr}(z, x)=r_{jr}(z, -x)$, $\tilde{r}_{ji}(z, x)=r_{ji}(z, -x)$, and the mirror symmetries $s_{jr}(z, x)=zr_{ji}(z, -x)$, $zs_{ji}(z, x)=r_{jr}(z, -x)$ [14, 15] are used.

For the lowest order $j=1$, $\phi_{0r}=1$ and $\phi_{0i}=0$. Substituting them into the linear equations (11), one obtains

$$\begin{aligned} r_1(z, x) &= k\left[x-\frac{1}{2}+\mathrm{i}2z\right]\exp\left[-\mathrm{i}\frac{1}{2}(2-a^2)z\right],\\ s_1(z, x) &= k\left[2z-\mathrm{i}\left(x+\frac{1}{2}\right)\right]\exp\left[\mathrm{i}\frac{1}{2}(2-a^2)z\right], \end{aligned} \tag{12}$$

with the arbitrary constant k.

From the recurrence formula (9), we have the first-order rational solution

$$\psi_1=\psi_0-\frac{4\mathrm{i}s_1 r_1^*}{|r_1|^2+|s_1|^2}=\left[-1+\frac{G_1+\mathrm{i}H_1}{D_1}\right]\exp[\mathrm{i}(2-a^2)z], \tag{13}$$

where $G_1=4$, $H_1=16z$, $D_1=1+4x^2+16z^2$.

In the next step, we solve the linear equations with the ψ function obtained at the previous step, $\psi=\psi_1$, to derive r_2, s_2. For the lowest order $j=2$, $\phi_{1r}=\dfrac{3-4x^2-16z^2}{1+4x^2+16z^2}$ and $\phi_{1i}=\dfrac{16z}{1+4x^2+16z^2}$. Inserting these expressions into linear equations (11), we obtain

$$r_{2r}(z,x)=p\frac{256z^4+96z^2-16x^4+16x^3+12x+192z^2x-3}{192D_1},$$
$$r_{2i}(z,x)=p\frac{16z^2-4x^3+3x-16z^2x+3}{12D_1},$$
$$s_{2r}(z,x)=zr_{2i}(z,-x)=p\frac{16z^3+4x^3z-3xz+16z^3x+3z}{12D_1},$$
$$s_{2i}(z,x)=\frac{r_{2r}(z,-x)}{z}=p\frac{256z^4+96z^2-16x^4-16x^3-12x-192z^2x-3}{192zD_1},\quad(14)$$

with the arbitrary constant p.

Thus, the recurrence formula (9) admits us to obtain the second-order rational solution

$$\psi_2=\psi_1-\frac{4is_2r_2^*}{|r_2|^2+|s_2|^2}=\left[1+\frac{G_2+iH_2}{D_2}\right]\exp[i(2-a^2)z],\quad(15)$$

where

$$G_2=36-15360z^4-3456z^2-192x^4-288x^2-4608z^2x^2,$$
$$H_2=z(720-12288z^4-1536z^2-768x^4+1152x^2-6144z^2x^2),$$
$$D_2=9+4096z^6+6912z^4+1584z^2+64x^6+48x^4+108x^2+3072z^4x^2+768z^2x^4-1152z^2x^2.$$

Similarly, substituting $j=3$, $\phi_{2r}=[64x^6+(768z^2-144)x^4+(-180+3072z^4-5760z^2)x^2+45-8448z^4+4096z^6-1872z^2]/D_2$ and $\phi_{2i}=[-768zx^4+(1152z-6144z^3)x^2+720z-1536z^3-12288z^5]/D_2$ into linear equations (11), one has

$$\begin{aligned}r_{3r}(z,x)=q[&512x^9-768x^8-(1536+24576z^2)x^6\\&+(576-18432z^2-49152z^4)x^5\\&+(-4320+46080z^2-122880z^4)x^4\\&+(2880+46080z^2+245760z^4-262144z^6)x^3\\&+(810+86400z^2-414720z^4-294912z^6-393216z^8)x\\&+589824z^8+1523712z^6+345600z^4\\&+25920z^2-135]/(25920D_2),\\r_{3i}(z,x)=q[&768x^8+(-1536+8192z^2)x^6-(2304+12288z^2)x^5\\&+(-1440-46080z^2+24576z^4)x^4\\&-(5760+98304z^4)x^3+(2160-103680z^2-258048z^4\\&-196608z^6)x-65536z^8-147456z^6+96768z^4\\&+54720z^2+1215]/(6480D_2),\end{aligned}\quad(16)$$

with the arbitrary constant q. Using these relations $s_{3r}(z,x)=zr_{3i}(z,-x)$, $s_{3i}(z,x)=\frac{r_{3r}(z,-x)}{z}$, we can obtain these expressions about $s_{3r}(z,x)$ and $s_{3i}(z,x)$. Inserting these expressions into the recurrence formula (9), the third-order rational solution reads

$$\psi_3=\psi_2-\frac{4is_3r_3^*}{|r_3|^2+|s_3|^2}=\left[-1+\frac{G_3+iH_3}{D_3}\right]\exp[i(2-a^2)z],\quad(17)$$

where $G_3=24576x^{10}+(92160+1474560z^2)x^8+(-1474560z^2+322560+19660800z^4)x^6+(-172800+2764800z^2-14745600z^4+110100480z^6)x^4+(-64800-20736000z^2+165888000z^4+165150720z^6+283115520z^8)x^2+276824064z^{10}+778567680z^8+215285760z^6-47001600z^4-777600z^2+16200$, $H_3=98304x^{10}z+(-368640z+1966080z^3)x^8+(-921600z-13762560z^3+15728640z^5)x^6+(-2073600z-11059200z^3-82575360z^5+62914560z^7)x^4+(1814400z-38707200z^3+168099840z^5-94371840z^7+125829120z^9)x^2+100663296z^{11}+157286400z^9-342097920z^7-236666880z^5-3801600z^3+453600z$, $D^3=4096x^{12}+(6144+98304z^2)x^{10}+(34560-368640z^2+983040z^4)x^8+(149760+552960z^2-2949120z^4+5242880z^6)x^6+(54000+3456000z^2-5529600z^4+3932160z^6+15728640z^8)x^4+(48600-2332800z^2+80179200z^4+221184000z^6+70778880z^8+25165824z^{10})x^2+16777216z^{12}+132120576z^{10}+244776960z^8+62668800z^6+36806400z^4+1490400z^2+2025$.

Note that these expressions (15) and (17) have different forms compared with second-order and third-order RWs of standard NLSE in [14] because there are arbitrary constant p in the expressions r_{2r}, r_{2i}, s_{2r} and s_{2i}, and arbitrary constant q in the expressions r_{3r}, r_{3i}, s_{3r} and s_{3i}.

Therefore, along this procedure, for any n-order, we can write the solution of (3) as follows

$$\psi_n=\left[(-1)^n+\frac{G_n+iH_n}{D_n}\right]\exp[i(2-a^2)z],\quad(18)$$

where G_n, H_n and D_n are polynomials in the two variables z and x, and they can be obtained from r_n and s_n by solving the linear equations (11).

From (2) and these expressions of ψ_n as (13), (15), (17) and (18), we can obtain RW solutions with the "high frequency" as $\{u_+, v_+\}$ and "low frequency" as $\{u_-, v_-\}$ of coupled NLSE (1). Note that multi-RWs have not been studied of system (1) although first-order RW (single RW) has been reported in [34].

Figure 1 exhibits the first-order, second-order and third-order RWs. Obviously, the solutions (11), (13) and (15) are symmetric about $z=0$ and $x=0$. Direct analysis

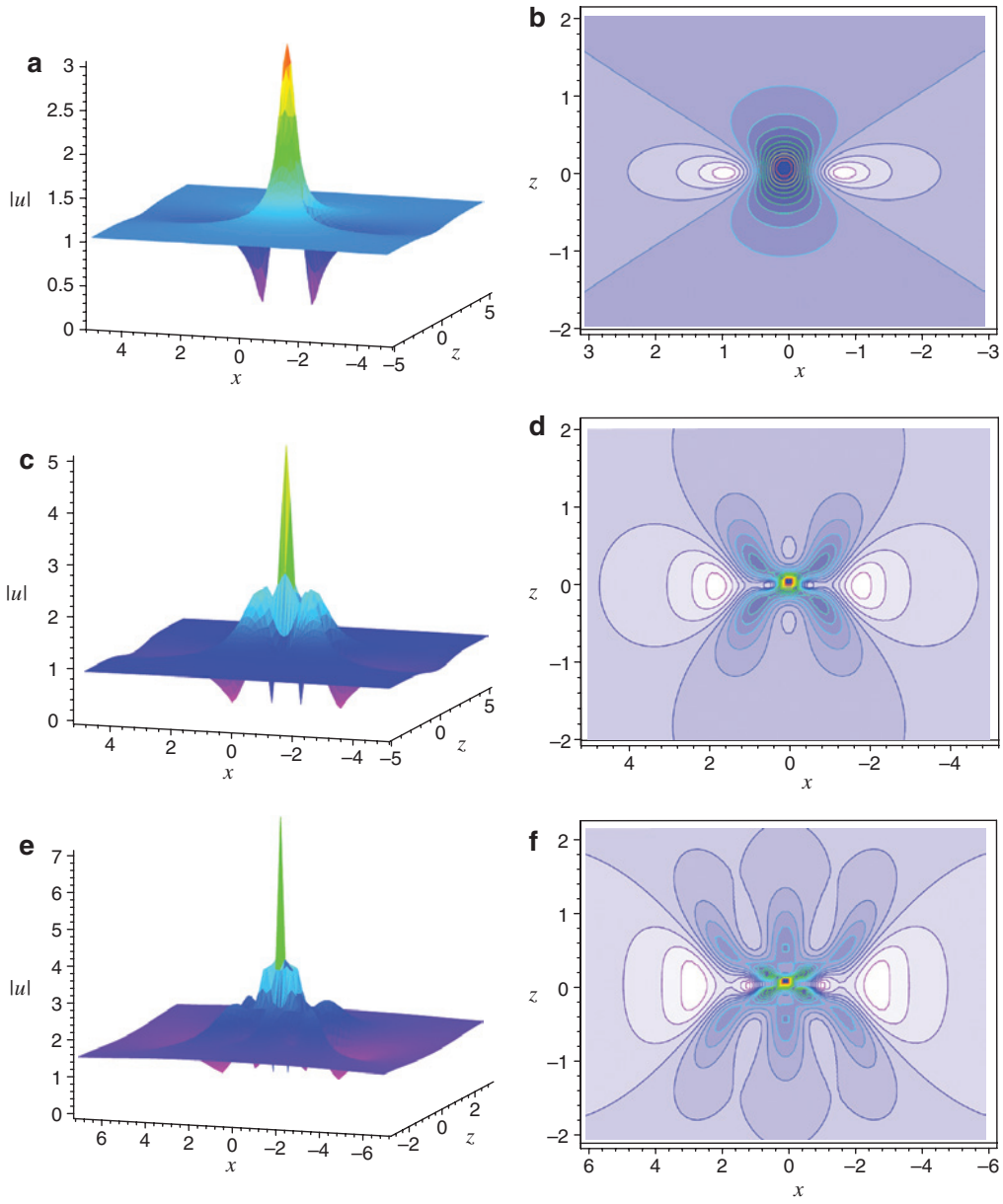

Figure 1: (Color online) (a), (c) and (e) The first-order, second-order and third-order RWs. (b), (d) and (f) Contour plots corresponding (a), (c) and (e).

shows that the background magnitude level of RWs is always 1, and the maximal values of these RWs are 3, 5 and 7 in Figure 1, respectively. The highest amplitude of the wave field reaches the values $2n+1$ for the n-order solution.

In [35], authors have reported that three first-order RWs, rather than just two, can construct the second-order rational solution. The reason is that the highest power of the denominator $d_n(z, x)$ of the nth-order rational solution is $n(n+1)$, and we can suppose that the general n-th order RW can be approximated as follows:

$$\psi_n = \left\{-1+4\sum_{k=1}^{n(n+1)/2}\frac{1+4\mathrm{i}(z-z_n)}{d_k}\right\}\exp\{\mathrm{i}(2-a^2)z\}, \qquad (19)$$

where the denominators are $d_k = 1+4(x-x_k)^2+16(z-z_k)^2$. There are $n(n+1)/2$ terms which produce $n(n+1)/2$ components in the complete solution. These related results have been presented in [35], thus we omit these similar discussions.

In [19], authors have been mentioned that first-order RW can be considered as a "quantum" to construct pattern structures of RW hierarchy including higher-order RWs

and breathers, etc. In next section, we construct breather solutions.

4 Breather Solutions and Structures

In order to illustrate the solving procedure more clearly, two linear functions in (8) can be re-written as $r=r_{nj}(z, x)$ and $s=s_{nj}(z, x)$ [36], where the subscript n is the order number and j is related to the eigenvalue λ_j. Note that different eigenvalues in the same order number are used to distinguish different lower order solutions. For example, when $n=1$, the single eigenvalue is λ_1 ($j=1$). When $n=2$, eigenvalues are λ_1 and λ_2 for $j=2$.

Along the procedure of [36], the seeding solution in a plane wave form is chosen as $u_0=\exp[\mathrm{i}(2-a^2)z]$ with the purely imaginary number λ. The compatibility of system (8) with $u=u_0$ leads to two linear functions r_{11} and s_{11} as

$$r_{11}=2\mathrm{i}\sin(A_{1r}+\mathrm{i}A_{1i})\exp\left[-\mathrm{i}\frac{1}{2}(2-a^2)z\right],$$
$$s_{11}=2\cos(B_{1r}+\mathrm{i}B_{1i})\exp\left[\mathrm{i}\frac{1}{2}(2-a^2)z\right], \tag{20}$$

with the subscripts r and i denoting real and imaginary parts, and $A_{1r}=\frac{1}{2}\left[\arccos\left(\frac{\kappa_1}{2}\right)+(x-x_1)\kappa_1-\frac{\pi}{2}\right]$, $B_{1r}=\frac{1}{2}\left[-\arccos\left(\frac{\kappa_1}{2}\right)+(x-x_1)\kappa_1-\frac{\pi}{2}\right]$, $A_{1i}=B_{1i}=(z-z_1)\kappa_1\sqrt{1-\frac{\kappa_1^2}{4}}$ and $\kappa_1=2\sqrt{1+\lambda_1^2}$. Here (z_1, x_1) are coordinate shifts.

The recurrence formula (9) yields the first-order breather solution

$$\psi_1=\psi_0+\frac{2(\lambda_1^*-\lambda_1)s_{11}r_{11}^*}{|r_{11}|^2+|s_{11}|^2}=\left[-1+\frac{L_1+\mathrm{i}M_1}{N_1}\right]\exp[\mathrm{i}(2-a^2)z], \tag{21}$$

where $L_1=2\kappa_1^2\cosh\delta_1(z-z_1)$, $M_1=4\kappa_1\nu_1\sinh\delta_1(z-z_1)$, $N_1=4[\cosh\delta_1(z-z_1)-\nu_1\cos\kappa_1(x-x_1)]$ with $\nu_1=\mathrm{Im}(\lambda_1)$ and $\delta_1=\nu_1\kappa_1$. When $0<\nu_1<1$, this solution (21) describe AB, and when $\nu_1>1$ (κ_1 is imaginary), this solution (21) describes KM soliton. Specifically, if $\nu_1\to 1$, this solution (21) can degenerate into the first-order rational solution (11) via the l'Hôpital's rule.

When we consider the second-order solution, two independent frequencies of modulation, κ_1 and κ_2, are combined in the solution via the next step of the DT. For a different eigenvalue λ_2, r_{12} and s_{12} are expressed as

$$r_{12}=2\mathrm{i}\sin(A_{2r}+\mathrm{i}A_{2i})\exp\left[-\mathrm{i}\frac{1}{2}(2-a^2)z\right],$$
$$s_{12}=2\cos(B_{2r}+\mathrm{i}B_{2i})\exp\left[\mathrm{i}\frac{1}{2}(2-a^2)z\right], \tag{22}$$

with $A_{2r}=\frac{1}{2}\left[\arccos\left(\frac{\kappa_2}{2}\right)+(x-x_2)\kappa_2-\frac{\pi}{2}\right]$, $B_{2r}=\frac{1}{2}\left[-\arccos\left(\frac{\kappa_2}{2}\right)+(x-x_2)\kappa_2-\frac{\pi}{2}\right]$, $A_{2i}=B_{2i}=(z-z_2)\kappa_2\sqrt{1-\frac{\kappa_2^2}{4}}$, and $\kappa_2=2\sqrt{1+\lambda_2^2}$ and coordinate shifts (z_2, x_2). Based on these linear functions s_{11}, r_{11}, s_{12} and r_{12}, the second-order ($n=2$) versions of the expressions r and s read [37]

$$r_{21}=\frac{(\lambda_1^*-\lambda_1)s_{11}^*r_{11}s_{12}+(\lambda_2-\lambda_1)|r_{11}|^2r_{12}+(\lambda_2-\lambda_1^*)|s_{11}|^2r_{12}}{|r_{11}|^2+|s_{11}|^2},$$
$$s_{21}=\frac{(\lambda_1^*-\lambda_1)s_{11}r_{11}^*r_{12}+(\lambda_2-\lambda_1)|s_{11}|^2s_{12}+(\lambda_2-\lambda_1^*)|r_{11}|^2s_{12}}{|r_{11}|^2+|s_{11}|^2}. \tag{23}$$

Therefore the second-order solution of NLSE (3) read

$$\psi_2=\psi_1+\frac{2(\lambda_2^*-\lambda_2)s_{21}r_{21}^*}{|r_{21}|^2+|s_{21}|^2}=\left[1+\frac{L_2+\mathrm{i}M_2}{N_2}\right]\exp[\mathrm{i}(2-a^2)z], \tag{24}$$

where $L_2=-\kappa_{12}[\kappa_1^2\delta_2\cosh(\delta_1Z_{s1})\cos(\kappa_2X_{s2})/\kappa_2-\kappa_2^2\delta_1\cosh(\delta_2Z_{s2})\cos(\kappa_1X_{s1})/\kappa_1-\kappa_{12}\cosh(\delta_1Z_{s1})\cosh(\delta_2Z_{s2})]$, $M_2=-2\kappa_{12}[\delta_1\delta_2\sinh(\delta_1Z_{s1})\cos(\kappa_2X_{s2})/\kappa_2-\delta_2\delta_1\sinh(\delta_2Z_{s2})\cos(\kappa_1X_{s1})/\kappa_1-\delta_1\sinh(\delta_1Z_{s1})\cosh(\delta_2Z_{s2})+\delta_2\cosh(\delta_1Z_{s1})\sinh(\delta_2Z_{s2})]$, $N_2=2(\kappa_1^2+\kappa_2^2)\delta_1\delta_2\cos(\kappa_1X_{s1})\cos(\kappa_2X_{s2})/(\kappa_1\kappa_2)-(2\kappa_1^2-\kappa_1^2\kappa_2^2+2\kappa_2^2)\cosh(\delta_1Z_{s1})\cosh(\delta_2Z_{s2})+4\delta_1\delta_2[\sin(\kappa_1X_{s1})\sin(\kappa_2X_{s2})+\sinh(\delta_1Z_{s1})\sinh(\delta_2Z_{s2})]-2\kappa_{12}[\delta_1\cos(\kappa_1X_{s1})\cosh(\delta_2Z_{s2})/\kappa_1-\delta_2\cos(\kappa_2X_{s2})\cosh(\delta_1Z_{s1})/\kappa_2]$ with $Z_{sj}=2(z-z_j)$, $X_{sj}=x-x_j$, $\delta_j=\kappa_j\sqrt{4-\kappa_j^2}/2$, $\kappa_{12}=\kappa_1^2-\kappa_2^2$, $\kappa_j=2\sqrt{1+\lambda_j^2}$, $j=1, 2$. Here κ is the modulation frequency, z_j and x_j determine the center of solution in $z-x$ coordinates.

When the values of $\mathrm{Im}(\lambda_1)$ and $\mathrm{Im}(\lambda_2)$ are both between 0 and 1, this solution (24) describe two ABs. When the values of $\mathrm{Im}(\lambda_1)$ and $\mathrm{Im}(\lambda_2)$ are both bigger than 1, this solution (24) describe two KM solitons. For the values of $\mathrm{Im}(\lambda_1)$ and $\mathrm{Im}(\lambda_2)$, When one of them is bigger than 1, and another is between 0 and 1, we can construct an AB and a KM soliton together.

Especially, when $\kappa_1\neq 0$ and $\kappa\to 0$, from solution (24), we can construct an AB or a KM soliton with a Peregrine soliton, and these expressions of L_2, M_2 and N_2 in solution (24) read

$$L_2 = \kappa\{\kappa[\kappa^2(4Z_{s2}^2 + 4X_{s2}^2 + 1) - 8]\cosh(\delta Z_{s1}) + 8\delta\cos(\kappa X_{s1})\}/8,$$
$$M_2 = \kappa\{8Z_{s2}[\delta\cos(\kappa X_{s1}) - \kappa\cosh(\delta Z_{s1})] + \delta\kappa(4Z_{s2}^2 + 4X_{s2}^2 + 1)\sinh(\delta Z_{s1})\}/4,$$
$$N_2 = -\{\delta[\kappa^2(4Z_{s2}^2 + 4X_{s2}^2 + 1) - 16]\cos(\kappa X_{s1}) + \kappa([\kappa^2(4Z_{s2}^2 + 4X_{s2}^2 - 3) + 16]\cosh(\delta Z_{s1}) - 16\delta[Z_{s2}\sinh(\delta Z_{s1}) + X_{s2}\sin(\kappa X_{s1})])\}/(4\kappa) \quad (25)$$

with $Z_{sj} = 2(z - z_j)$, $X_{sj} = x - x_j$, $\delta = \kappa\sqrt{4 - \kappa^2}/2$, $\kappa = 2\sqrt{1 + \lambda_1^2}$, $j = 1, 2$. When $0 < \mathrm{Im}(\lambda_1) < 1$ and $\mathrm{Im}(\lambda_1) > 1$ in solution (25), the PS combined by AB and KM soliton can be built up, respectively.

In order to obtain higher order solution, higher order versions of these expressions for r and s can be defined as [37]

$$r_{nm} = \frac{(\lambda_{n-1}^* - \lambda_{n-1})s_{n-1,1}^* r_{n-1,1} s_{n-1,m+1} + (\lambda_{m+n+1} - \lambda_{n-1})|r_{n-1,1}|^2 r_{n-1,m+1} + (\lambda_{m+n-1} - \lambda_{n-1}^*)|s_{n-1,1}|^2 r_{n-1,m+1}}{|r_{n-1,1}|^2 + |s_{n-1,1}|^2},$$
$$s_{nm} = \frac{(\lambda_{n-1}^* - \lambda_{n-1})s_{n-1,1} r_{n-1,1}^* s_{n-1,m+1} + (\lambda_{m+n+1} - \lambda_{n-1})|s_{n-1,1}|^2 s_{n-1,m+1} + (\lambda_{m+n-1} - \lambda_{n-1}^*)|r_{n-1,1}|^2 s_{n-1,m+1}}{|r_{n-1,1}|^2 + |s_{n-1,1}|^2}. \quad (26)$$

Here the subscript m is used purely for enumeration. For such, the third order function r_{31} can be determined by the second-order functions r_{21}, s_{21}, r_{22} and s_{22}, which are related to the first-order functions r_{11}, s_{11}, r_{12}, s_{12}, r_{13} and s_{13}.

Therefore, the n-order solution can be obtained from the following recursion

$$\psi_n = \psi_{n-1} + \frac{2(\lambda_n^* - \lambda_n)s_{n1} r_{n1}^*}{|r_{n1}|^2 + |s_{n1}|^2} = \left[(-1)^n + \frac{L_n + \mathrm{i}M_n}{N_n}\right]\exp[\mathrm{i}(2 - a^2)z], \quad (27)$$

where L_n, M_n and N_n can be generated from the above procedure.

From (2) and these expressions of ψ_n as (21), (24), (25) and (27), we can obtain breather solutions with the "high frequency" as $\{u_+, v_+\}$ and "low frequency" as $\{u_-, v_-\}$ of coupled NLSE (1). Note that these second-order breather solutions have not been reported in the system without $\mathcal{PT}$-symmetric terms.

Two-breather solution (24) can describe two-KM solitons, two-ABs and an AB and an KM soliton by choosing different values of λ_1 and λ_2 [x-periodic and z-localised structure]. Figure 2 displays three kinds of two-ABs and three kinds of superposed ABs. The white lines separate Figure 2 into the left and right regions with the same structures. For long periods, the AB can be considered as chains of Peregrine soliton peaks in x-direction and z-localised structure. Figure 2a, c and e are all two parallel ABs built from first-order RW-like structures. The number of RWs in two-ABs is decided by the ratio κ_1:κ_2.

At first, we discuss two-ABs [x-periodic and z-localised structure]. The white lines separate Figure 2a and b into the left and right regions with the same structures. The conformation from Figure 2a and b displays the process for the superposition when κ_1:κ_2 = 3:1. In Figure 2a, two RWs in the array with the smaller value of z and a RW in the array with the bigger value of z triangularly arrange and form a triplet, and another RW in the array with the smaller value of z has no counterpart in another array. The triplet merges into a second-order RW and the pair-less RW remains the first-order RW when they share the same origin, and the superposed AB is constructed in Figure 2b. This superposed AB produces as a chain of the second-order RW-like structure alternating with the first-order RW-like structures.

When κ_1:κ_2 = 2:3, the ratio of the numbers of RWs in two arrays of KM solitons is also 2:3 (Figure 2c). In the left or right region of Figure 2c, there are five first-order RW-like structures. When they share the same origin, the quin-RW-like structure produce. In Figure 2d, the superposed AB is a series of quin-RWs which are localised in z-axis and periodic in x-axis.

When the ratio of κ_1 and κ_2 has other values, we can also construct other structures. For example, κ_1:κ_2 = 1:2, in Figure 2f, the superposed AB is a chain of triplets which build from three first-order RWs in Figure 2e.

These superposed two-AB structures are firstly reported although some nonlinear superposition of two ABs for standard NLSE has also been studied in [36]. Similar structures repeating along the x axis appear in the AB cases, although the integer ratios in this situation must be applied to δ_1:δ_2. For the length of limit, we omit their structures.

Besides two-ABs and two-KM solitons, we can also discuss a AB crossing a KM soliton when one of the values of Im (λ_2) and Im (λ_2) is between 0 and 1, and another is bigger than 1. Figure 3 demonstrates two cases of ABs crossing KM solitons. In Figure 3a, the crossing location is between two RWs of KM soliton, thus AB and KM soliton intersect without interaction. In Figure 3b, one of RWs in KM soliton interact with the AB in the intersection, thus a

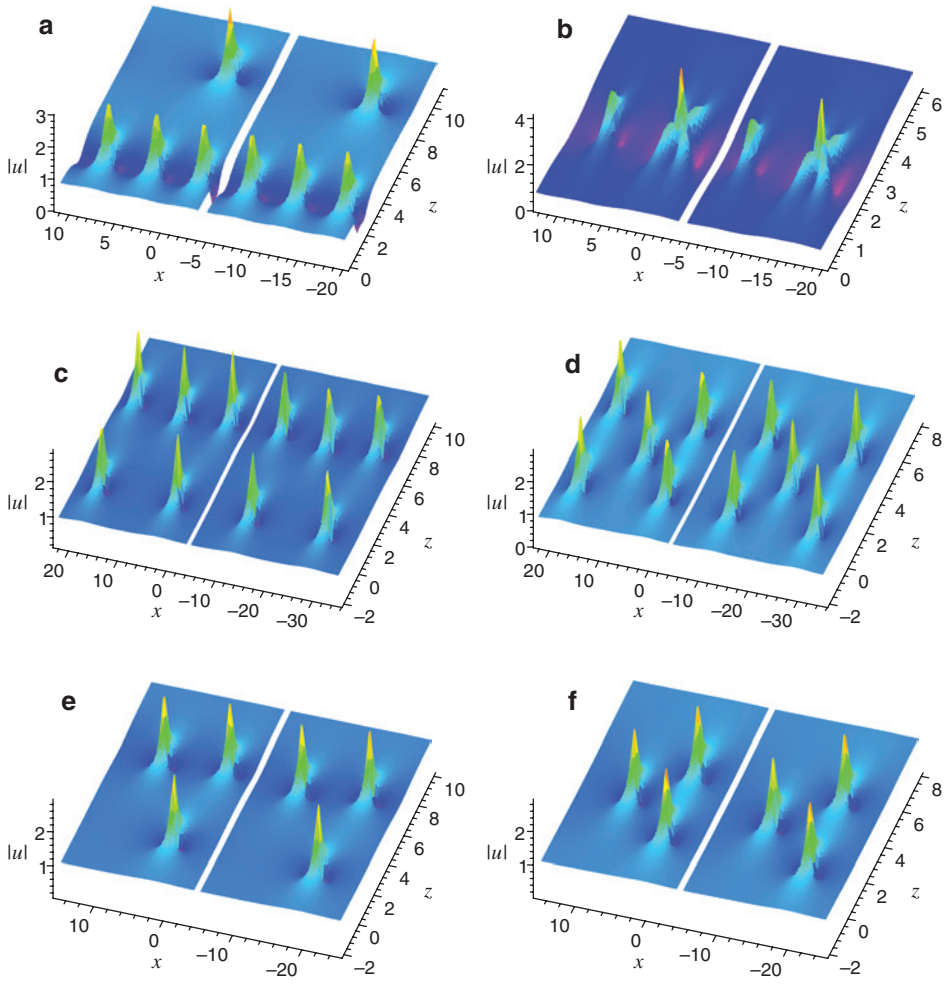

Figure 2: (Color online) (a), (c) and (e) three kinds of two-ABs, and (b), (d) and (f) three kinds of superposed ABs. Parameters are chosen as (a) $\kappa_1=1.2$, $\kappa_2=0.4$, $z_1=5$, $z_2=15$, $x_1=x_2=0$, (b) $\kappa_1=1.2$, $\kappa_2=0.4$, $z_1=z_2=5$, $x_1=x_2=0$, (c) $\kappa_1=0.4$, $\kappa_2=0.6$, $z_1=5$, $z_2=10$, $x_1=2$, $x_2=4$, (d) $\kappa_1=0.4$, $k_2=0.6$, $z_1=z_2=5$, $x_1=2$, $x_2=4$, (e) $\kappa_1=0.3$, $\kappa_2=0.6$, $z_1=5$, $z_2=10$, $x_1=2$, $x_2=4$ and (f) $\kappa_1=0.3$, $\kappa_2=0.6$, $z_1=z_2=5$, $x_1=2$, $x_2=4$.

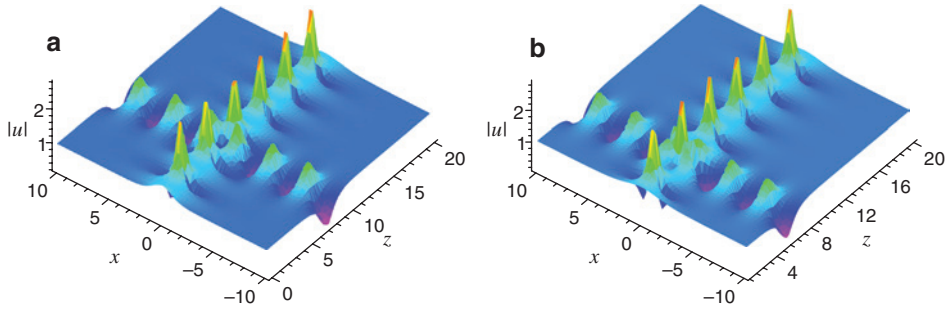

Figure 3: (Color online) Two kinds of AB crossing KM soliton. Parameters are chosen as (a) $z_2=15$ and (b) $z_2=11$ with $\lambda_1=1.1i$, $\lambda_2=0.4i$, $z_1=5$, $x_1=x_2=0$.

second-order RW appears in the crossing location, which is firstly reported although the crossing AB and KM soliton for standard NLSE in Figure 1a has been studied in [36]. This difference of structures originates from the different shifts z_2 of KM solitons in two cases. Thus we can modulate this parameter to construct different structures.

At last, we discuss the PS combined by AB and KM soliton from solution (25). Here we give a nonlinear superposition structure of an AB with a PS in Figure 4, where the PS is parallel with the AB, and they are separated. Moreover, the PS is embedded in the AB can be also constructed like in [36].

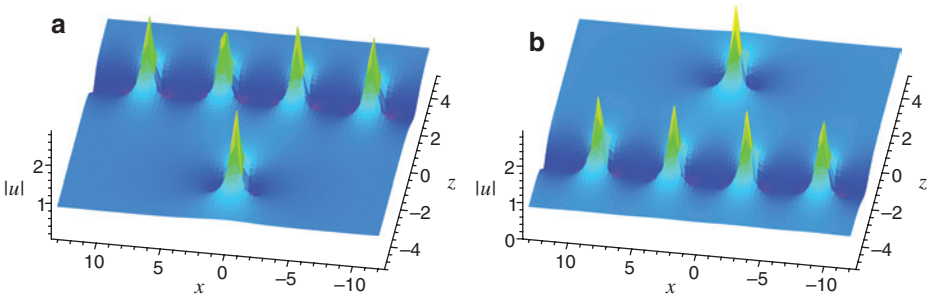

Figure 4: The combined PS and AB for solution (25): (a) Shifts are $z_1 = -z_2 = 4$, (b) shifts are $z_1 = -z_2 = -4$ with $x_1 = x_2 = 0$.

5 Conclusions

In conclusion, via the modified DT method, starting from zero solution and the plane wave solution, the hierarchies of rational solutions and breather solutions with "high frequency" and "low frequency" of the coupled NLSE in parity-time symmetric nonlinear couplers with gain and loss are constructed, respectively. From these results, some basic characteristics of multi-RWs and multi-breathers are studied. Based on the property of RW as the "quantum" of pattern structure in RW hierarchy, we further study the novel structures of the superposed ABs, KM solitons and their combined structures.

Note that we only consider the case with the same Kerr nonlinearity coefficient of both the waveguides. If there is a slight mismatch between the Kerr nonlinearity coefficient of the two waveguides, it is difficult to transform a coupled NLSE into a single NLSE. Therefore, exact multi-RWs and multi-breathers can not be derived. In this case, we can use direct numerical simulation to study how the propagation of the RWs will be affected by mismatched Kerr nonlinearity. This issue requires a separate report (in preparation).

References

[1] Y. P. Zhang and C. Q. Dai, Z. Naturforsch. A **70**, 835 (2015).
[2] L. Q. Kong and C. Q. Dai, Nonlinear Dyn. **81**, 1553 (2015).
[3] C. Q. Dai and Y. J. Xu, Appl. Math. Model. **39**, 7420 (2015).
[4] Y. Y. Wang and C. Q. Dai, Nonlinear Dyn. **83**, 1331 (2016).
[5] Y. Y. Wang and C. Q. Dai, Appl. Math. Model. **40**, 3475 (2016).
[6] W. J. Liu, L. H. Pang, H. N. Han, W. L. Tian, H. Chen, et al., Opt. Exp. **20**, 26023 (2015).
[7] W. J. Liu, L. H. Pang, H. N. Han, Z. W. Shen, M. Lei, et al., Photon. Res. **3**, 111 (2016).
[8] C. Q. Dai, Y. Wang, J. Liu, Nonlinear Dyn. **84**, 1157 (2016).
[9] W. J. Broad, Rogue Giants at Sea, The New York Times, New York 2006.
[10] C. Q. Dai and Y. Y. Wang, Nonlinear Dyn. **80**, 715 (2015).
[11] Y. Y. Wang, J. T. Li, C. Q. Dai, X. F. Chen, and J.F. Zhang, Phys. Lett. A **377**, 2097 (2013).
[12] J. F. Zhang and C. Q. Dai, Acta. Phys. Sin. **65**, 050501 (2016).
[13] D. H. Peregrine, J. Austral. Math. Soc. Ser. B. **25**, 16 (1983).
[14] N. Akhmediev, A. Ankiewicz, and J. M. Soto-Crespo, Phys. Rev. E. **80**, 026601 (2009).
[15] A. Ankiewicz, J. M. Soto-Crespo, and N. Akhmediev, Phys. Rev. E. **81**, 046602 (2010).
[16] E. A. Kuznetsov, Dokl. Akad. Nauk SSSR **236**, 575 (1977).
[17] Y. C. Ma, Stud. Appl. Math. **60**, 43 (1979).
[18] N. Akhmediev and V. I. Korneev, Theor. Math. Phys. **69**, 1089 (1986).
[19] D. J. Kedziora, A. Ankiewicz, and N. Akhmediev, Phys. Rev. E. **88**, 013207 (2013).
[20] C.Q. Dai, Y.Y. Wang, and X. F. Zhang, Opt. Express. **22**, 29862 (2014).
[21] L. Wang, X. Li, F. H. Qi, and L. L. Zhang, Ann. Phys. **359**, 97 (2015).
[22] X. Y. Xie, B. Tian, Y. F. Wang, Y. Sun, and Y. Jiang, Ann. Phys. **362**, 884 (2015).
[23] C. M. Bender and S. Boettc, Phys. Rev. Lett. **80**, 5243 (1998).
[24] Z. H. Musslimani, K. G. Makris, R. El-Ganainy, and D. N. Christodoulides, Phys. Rev. Lett. **100**, 030402 (2008).
[25] C. Q. Dai and Y. Y. Wang, Nonlinear Dyn. **83**, 2453 (2016).
[26] A. A. Sukhorukov, Z. Xu, and Y. S. Kivshar, Phys. Rev. A. **82**, 043818 (2010).
[27] I. V. Barashenkov, S. V. Suchkov, A. A. Sukhorukov, S. V. Dmitriev, and Y. S. Kivshar, Phys. Rev. A. **86**, 053809 (2012).
[28] Y. X. Chen, Y. F. Jiang, Z. X. Xu, and F. Q. Xu, Nonlinear Dyn. **82**, 589 (2015).
[29] N. V. Alexeeva, I. V. Barashenkov, A. A. Sukhorukov, and Y. S. Kivshar, Phys. Rev. A. **85**, 063837 (2012).
[30] F. K. Abdullaev, V. V. Konotop, M. Ögren, and M. P. SØrensen, Opt. Lett. **36**, 4566 (2011).
[31] S. V. Suchkov, B. A. Malomed, S. V. Dmitriev, and Y. S. Kivshar, Phys. Rev. E. **84**, 046609 (2011).
[32] R. Driben and B. A. Malomed, Opt. Lett. **36**, 4323 (2011).
[33] C. E. Ruter, K. G. Makris, R. El-Ganainy, D. N. Christodoulides, M. Segev, et al., Nature Phys. **6**, 192 (2010).
[34] Y. V. Bludov, R. Driben, V. V. Konotop, and B. A. Malomed, J. Opt. **15**, 064010 (2013).
[35] A. Ankiewicz, D. J. Kedziora, and N. Akhmediev, Phys. Lett. A. **375**, 2782 (2011).
[36] D. J. Kedziora, A. Ankiewicz, and N. Akhmediev, Phys. Rev. E. **85**, 066601 (2012).
[37] D. J. Kedziora, A. Ankiewicz, and N. Akhmediev, Phys. Rev. E. **84**, 056611 (2011).